

● *Original Contribution*

## DUAL LUMEN TRANSDUCER PROBES FOR REAL-TIME 3-D INTERVENTIONAL CARDIAC ULTRASOUND

WARREN LEE,\* SALIM F. IDRIS,† PATRICK D. WOLF\* and STEPHEN W. SMITH\*

\*Department of Biomedical Engineering, Duke University, Durham, NC, USA; and †Department of Pediatrics, Duke University Medical Center, Durham, NC, USA

(Received 12 December 2002; revised 28 March 2003; in final form 8 April 2003)

**Abstract**—We have developed dual lumen probes incorporating a forward-viewing matrix array transducer with an integrated working lumen for delivery of tools in real-time 3-D (RT3-D) interventional echocardiography. The probes are of 14 Fr and 22 Fr sizes, with 112 channel 2-D arrays operating at 5 MHz. We obtained images of cardiac anatomy and simultaneous interventional device delivery with an *in vivo* sheep model, including: manipulation of a 0.36-mm diameter guidewire into the coronary sinus, guidance of a transseptal puncture using a 1.2-mm diameter Brockenbrough needle, and guidance of a right ventricular biopsy using 3 Fr biopsy forceps. We have also incorporated the 22 Fr probe within a 6-mm surgical trocar to obtain apical four-chamber ultrasound (US) scans from a subcostal position. Combining the imaging catheter with a working lumen in a single device may simplify cardiac interventional procedures by allowing clinicians to easily visualize cardiac structures and simultaneously direct interventional tools in a RT3-D image. (E-mail: warren.lee@duke.edu)  
© 2003 World Federation for Ultrasound in Medicine & Biology.

**Key Words:** 2-D array, Volumetric ultrasound imaging, Intracardiac echocardiography, Forward-viewing catheter.

### INTRODUCTION

The increasing variety of interventional cardiac procedures developed in recent years has underscored the requirement for an imaging method that offers satisfactory visualization of cardiac structures and interventional devices. Many of these procedures, such as catheter-based electrophysiological mapping and ablation, are conventionally performed under fluoroscopic guidance. However, the inability to image soft tissue structures using fluoroscopy, as well as the risks of prolonged exposure to ionizing radiation, have motivated a search for alternative imaging modalities to guide these interventional procedures.

Recent innovations in the field of minimally invasive cardiac surgical procedures have also prompted the need for improved visualization and guidance. New procedures, such as left ventricular or biventricular pacing for the treatment of congestive heart failure, have shown impressive results in reduced morbidity and improved quality of life (Abraham et al. 2002a, 2002b). However, these pacing methods require the placement of leads

within or on the right ventricle (RV) and left ventricle (LV) (Izutani et al. 2002). These procedures would benefit from the ability to better visualize both the pacemaker lead and its contact with the cardiac structure. Minimally invasive surgical procedures have also been developed for coronary artery bypass grafts, aortic and mitral valve surgery and repair of atrial septal defects. These procedures require monitoring of cardiac function, such as cardiac output and ejection fraction, both during surgery and postoperatively. Such long-term monitoring and measurements are conventionally performed using 2-D transesophageal echocardiography (TEE).

Intracardiac echocardiography (ICE) is an imaging method that has been shown in recent studies to be useful in guiding interventional procedures where transthoracic echocardiography (TTE) and TEE are less favorable (Bartel et al. 2002). Intracardiac transducers are built on catheters that are directed into the cardiac chambers and vessels. There are several advantages of the intracardiac approach over the transthoracic approach. One of these advantages is a consequence of the reduced scan depth, which allows a higher operating frequency and resultant improvement in resolution. Intracardiac echo also resolves problems that may arise using TTE due to poor

Address correspondence to: Warren Lee, Box 90281, Duke University, Durham, NC 27708 USA. E-mail: warren.lee@duke.edu

acoustic windows. Until recently, ICE was limited to 2-D monoplanar scanning acquired by rotating a circularly scanned piston transducer (Chu et al. 1994), or using 1-D phased-array US catheters (Bruce et al. 1999). These devices have shown promise imaging interventional cardiac procedures, but have intrinsic limitations associated with 2-D scanning to guide interventional devices that are manipulated in 3-D.

During the past several years, real-time 3-D (RT3-D) US imaging has gained increasing utility in the field of cardiology. Originally developed at Duke University by von Ramm and Smith (Smith et al. 1991; von Ramm et al. 1991), RT3-D echocardiography addresses the inherent limitations associated with conventional imaging techniques such as monoplanar US and fluoroscopy. Recent studies have demonstrated the effectiveness of RT3-D echocardiography for the monitoring of left ventricular function (Schmidt et al. 1999), detection of perfusion defects (Camarano et al. 2002), reduced scanning times in dobutamine stress echo examinations (Ahmad et al. 2001), guidance of RV endomyocardial biopsy (McCreery et al. 2001), measurement of peak LV flow velocities (Tsujino et al. 2001) and evaluation of congenital cardiac abnormalities (Fleishman et al. 1996).

In RT3-D echocardiography, a 2-D matrix array transducer is used to steer and focus the US beam throughout a 3-D volume. Within the acquired volume of data, multiple real-time, simultaneous B and C scans are displayed as well as RT3-D rendered volumes, 3-D pulse-wave Doppler and 3-D color flow Doppler.

The miniaturization of these 2-D matrix-array transducers has made RT3-D ICE possible. We have previously described several matrix-array, side-viewing catheter configurations including a 5-MHz, 12-Fr design (Light et al. 2001; Smith et al. 2002) and a 7-MHz, 9-Fr design (Lee and Smith 2002). We discussed the feasibility of using these catheters as stand-alone imaging devices for the guidance of interventional electrophysiology. In this paper, we describe the design, fabrication and testing of forward-viewing, dual-lumen catheter configurations allowing RT3-D ICE and simultaneous interventional tool delivery and visualization in a single device. By combining the forward-viewing transducer probe with a working lumen, a clinician may first identify the tissue region to be treated and then, predictably, deliver the interventional device while imaging the entire process in real-time 3-D. This forward-viewing integrated device may result in a simplification of interventional procedures over those guided using a side-viewing catheter transducer, where the interventional device must be positioned independently of the imaging device, and delivery of the interventional device is not as predictable as when they are prealigned.

The devices are of 14-Fr and 22-Fr catheter sizes, with 112-channel matrix-array transducers operating at 5 MHz. We have utilized these devices to guide cardiac interventions in the *in vivo* sheep model including manipulation of a 0.36-mm (0.014") diameter guidewire into the coronary sinus, which is a prelude to the introduction of over-the-wire pacing leads into the coronary sinus for procedures such as biventricular pacing (Blanc et al. 1997). We also used them to guide transseptal puncture using a 1.2-mm diameter Brockenbrough needle (Daig Corporation, Minnetonka, MN), a procedure frequently used to gain access to the left atrium in the course of radiofrequency (RF) catheter ablation of arrhythmogenic sites in the pulmonary veins (Lesh et al. 2000). In addition, they were used for guidance of an RV biopsy using a 3-Fr biopsy forceps (Pentax Medical Corporation, Orangeburg, NY), useful in the diagnosis of rejection in cardiac allograft recipients (Caves et al. 1974). We have also used the 22-Fr device to obtain apical four-chamber views using a surgical trocar to position the catheter subcutaneously from a subcostal approach. From this position, it may be possible to monitor cardiac function and to evaluate the effectiveness of the site of biventricular pacemaker lead placement during surgery. It may also be possible to monitor cardiac function with minimal invasiveness during cardiac surgery and in the postoperative period.

## METHODS

### *Real-time three-dimensional ultrasound system*

We used the model 1 commercial US system (Volumetrics Medical Imaging, Durham, NC) to acquire 3-D pyramidal scans in real-time. The system has up to 512 transmit and 256 receive channel capabilities, and employs 16:1 parallel receive mode processing to generate 4100 B-mode lines at a maximum rate of 60 volumes/s. Two B-mode images and up to three C-mode images are displayed simultaneously. These images can be tilted at any angle and positioned to any depth within the pyramidal scan volume. The system can also display RT3-D rendered volumes by integrating and spatially filtering the data between two user-selected C-mode planes. Figure 1 shows the 14-Fr forward-viewing catheter with tool port, as well as a schematic of the scanned pyramidal volume and display planes.

### *Transducer fabrication*

The transducers used in this study operate at 5 MHz, with 112 active elements in a  $10 \times 14$  matrix, arranged in the pattern shown in Fig. 2. The simulated azimuth and elevation acoustic beam profiles were obtained using Field II software (Jensen and Svendsen 1992), assuming a Gaussian-shaped excitation centered at 5 MHz with a

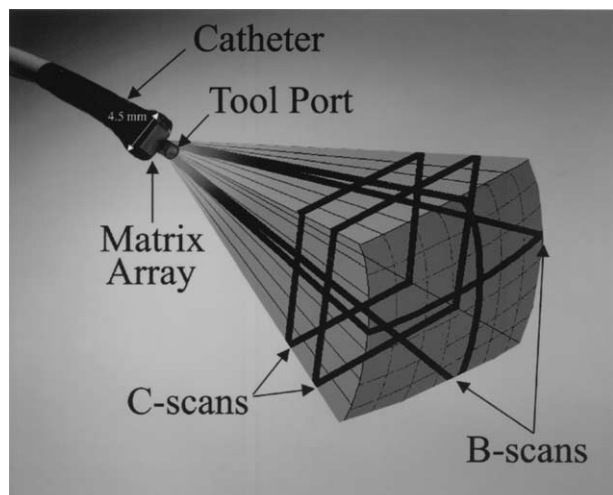


Fig. 1. The 14-Fr forward-viewing matrix-array catheter with tool port, showing acquired pyramidal volume of data and display planes. By integrating and spatially filtering between the C-planes, a 3-D rendered image is displayed in real-time.

–6-dB fractional band width of 30%. Figure 3A and B shows the simulated acoustic beam vs. angle, indicating a –6-dB beam width of  $12^\circ$  in azimuth, and  $8.7^\circ$  in elevation. Figure 3C and D shows the –6-dB and –20-dB contours of the beam width in mm vs. depth out to 60 mm. By using the –6-dB beam width as an

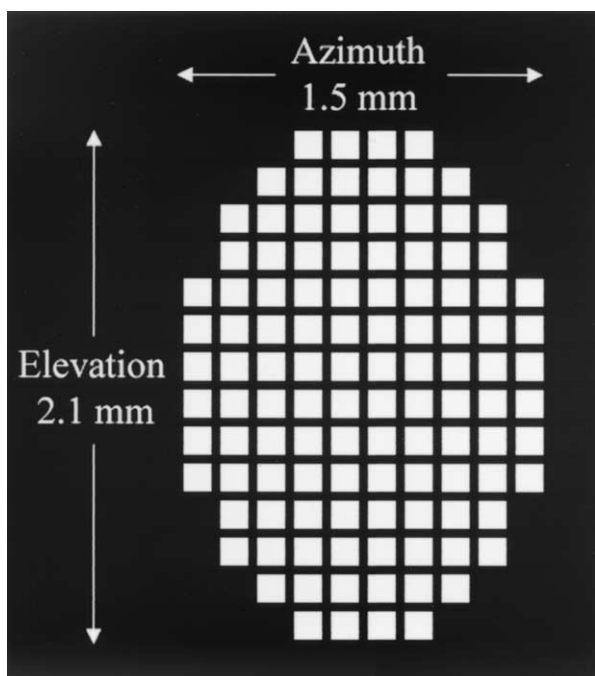


Fig. 2. Matrix-array pattern showing aperture sizes in azimuth and elevation dimensions.

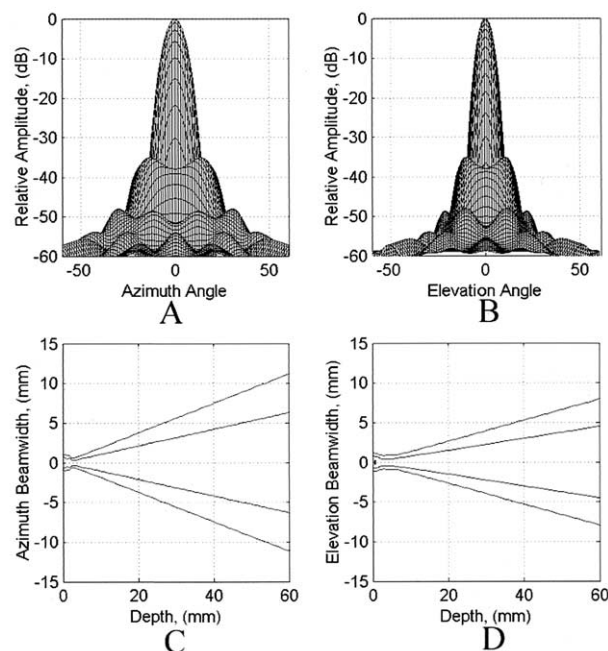


Fig. 3. Simulated beam plots of the transducer. (A) Azimuth and (B) elevation beam plots vs. angle. (C) –6 and (D) –20-dB contours of the azimuth and elevation beam width in mm vs. depth to 60 mm.

estimate of lateral resolution, Fig. 3C and D shows that, at a depth of 30 mm, the transducer has a lateral resolution of 6.3 mm and 4.5 mm in the azimuth and elevation directions, respectively. Due to the wide angular beam width of these interventional cardiac transducers, we modified the Volumetrics 3-D scanner to display a selectable field of view of  $65^\circ$ ,  $90^\circ$  or  $120^\circ$ , with a maximum receive-mode angular sampling interval of  $2^\circ$ .

The transducers were constructed on a multilayer flexible interconnect circuit (MicroConnex, Snoqualmie, WA) with methods previously described (Fiering *et al.* 2000). The flex circuit is shown in Fig. 4A, and a closeup of the diced array is shown in Fig. 4B. The transducer was then attached to a triangular shaped acoustic backing of loaded epoxy, shown in Fig. 5. A ribbon-based cable (Microflat, W.L. Gore & Associates) was fed through an 8-Fr catheter lumen and the distal end of the cable was terminated onto the solder pads of the flex circuit. The proximal end of the ribbon cable was terminated to a connector leading to the system cable of the scanner. The 14-Fr catheter was completed by using a cyanoacrylate to bond a 1.3-mm diameter polyimide tube to the 8-Fr imaging catheter. The polyimide tubing served as the working lumen through which the interventional tools were delivered. The 22-Fr catheter was completed by juxtaposing a 9-Fr working lumen with the 8-Fr imaging catheter and sealing the assembly with a heat-shrinkable

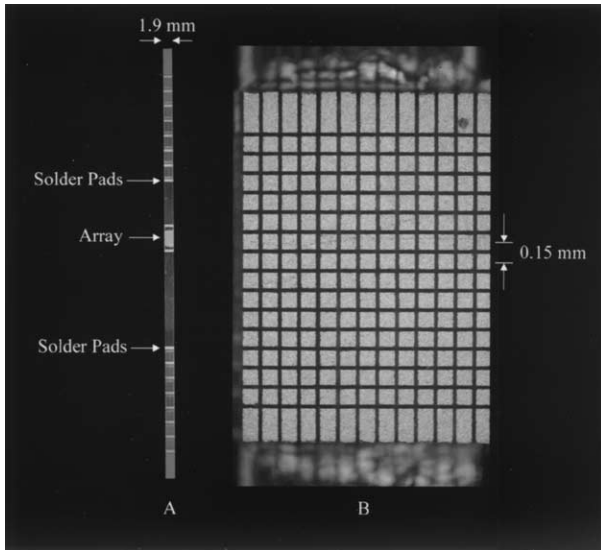


Fig. 4. (A) Multilayer flexible interconnect circuit showing the array and solder pads. (B) Closeup of the diced array. The interelement spacing is 0.15 mm, the saw kerf is 0.025 mm and the elements are 0.125 mm on a side.

polyolefin tube. Figure 6 shows a photograph of the completed intracardiac transducers, including the 14-Fr dual-lumen forward-viewing array in Fig. 6A, and the 22-Fr dual-lumen forward-viewing array inserted into a 6-mm diameter surgical trocar in Fig. 6B.

*Measurements*

The impulse response and power spectrum were measured to characterize the transducer. The impulse response was obtained by transmitting with a Panametrics Model 5073PR (Waltham, MA) pulser/receiver, and observing the reflection from an aluminum block with a Tektronix model TDS744A digitizing oscilloscope (Wilsonville, OR). The spectrum was obtained using a Panametrics 5605A Stepless Gate and a Hewlett-Packard model 3588A spectrum analyzer (Palo Alto, CA).

*Animal model*

The *in vivo* images in this study were acquired using a sheep model. The study was approved by the Institutional Animal Care and Use Committee at Duke University and conformed to the Research Animal Use Guidelines of the American Heart Association. A total of 15 to 22 mg/kg of IM injected ketamine hydrochloride was used to sedate the animals. A 20-gauge IV catheter was placed in the saphenous vein for the purpose of IV fluid administration, and the animal was placed on a water-heated thermal pad. The animals were mechanically ventilated with 95 to 99% oxygen and 1 to 5% isoflurane for anesthesia. A nasogastric tube was passed to the stomach

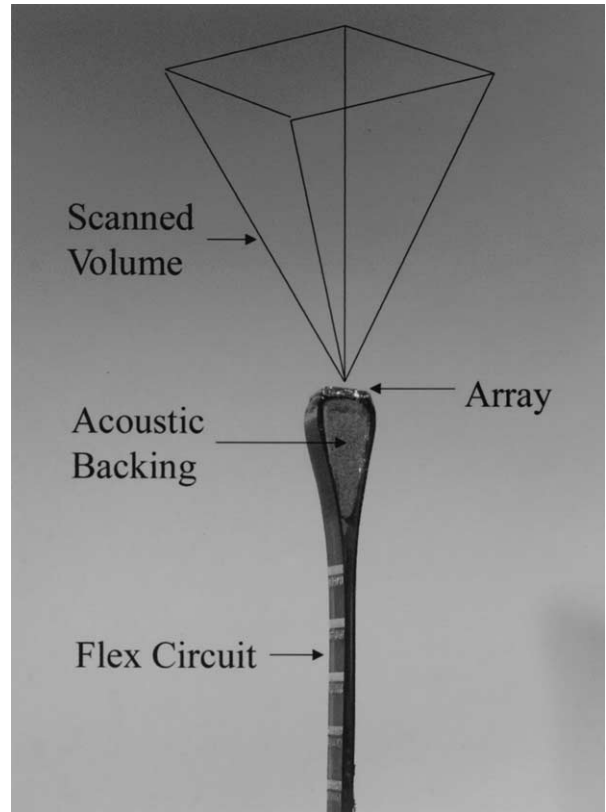


Fig. 5. Photograph of the flex circuit attached to an acoustic backing, showing the forward-viewing orientation of the array. The pyramidal scanned volume is shown schematically on the photograph for reference.

to prevent rumenal typany. A femoral arterial line was placed on the left side *via* a percutaneous puncture, and electrolyte and respirator adjustments were made based

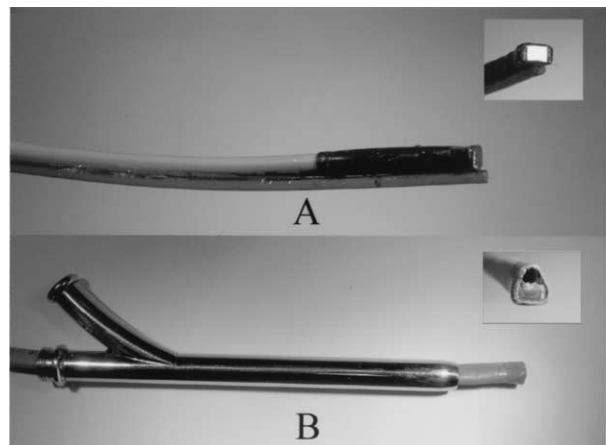


Fig. 6. Photograph of the completed dual lumen US probes. (A) 14-Fr forward-viewing with tool port; inset = closeup of transducer face. (B) 22-Fr forward-viewing with tool port in surgical trocar; inset = closeup of transducer face.

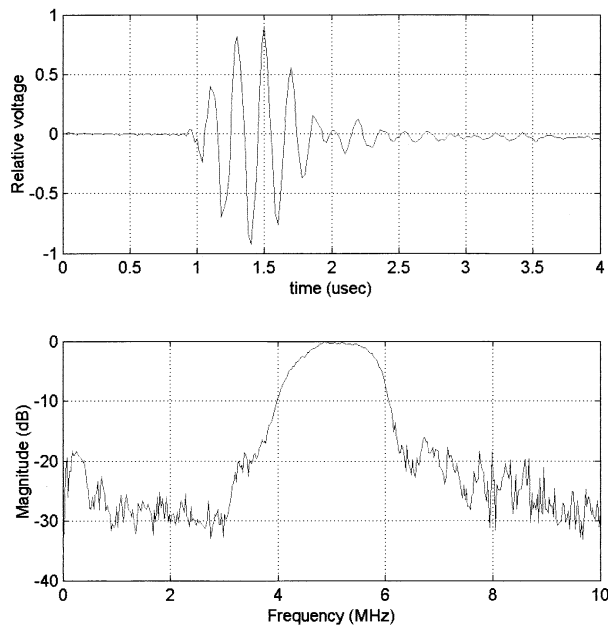


Fig. 7. Illustrative impulse response and spectrum. The transducer has  $-6$ -dB and  $-20$ -dB pulse lengths of 0.63 and 1.31  $\mu$ s, respectively. The center frequency is 5.0 MHz and the  $-6$ -dB fractional band width is 36%.

on serial electrolyte and arterial blood gas measurements. Sodium chloride (0.9%) was continuously infused using an IV maintenance fluid. Throughout the procedure, blood pressure, lead II ECG and temperature were continuously monitored. For the open chest procedures, the heart was exposed by median sternotomy.

#### *Intracardiac echocardiography*

We used both open- and closed-chest sheep models to obtain our images. Use of the open-chest model allowed confirmation of the relative locations and orientations of the transducer probe with respect to the cardiac structures imaged by manual palpation, and the closed-chest experiments demonstrated the capability of utilizing the transducers in a more clinically relevant setting. The images shown include user-selected B-scans, C-scans and rendered volumes. In those figures where C-scans are shown, the C-scan plane is defined by arrows on either side of the B-scans. In those figures where rendered images are shown, the rendered volume is defined by the data in between the arrows that are at the side of (or below) the B-scans. For a schematic drawing of the B-scans, C-scans and rendered volumes, refer to Fig. 1. White dots on the right side of the B-scans indicate 1-cm depth increments. It should be noted that the scales for the B-scans do not correspond to the rendered images and, also, that the rendered images should not, in general, be used for measurements. In the

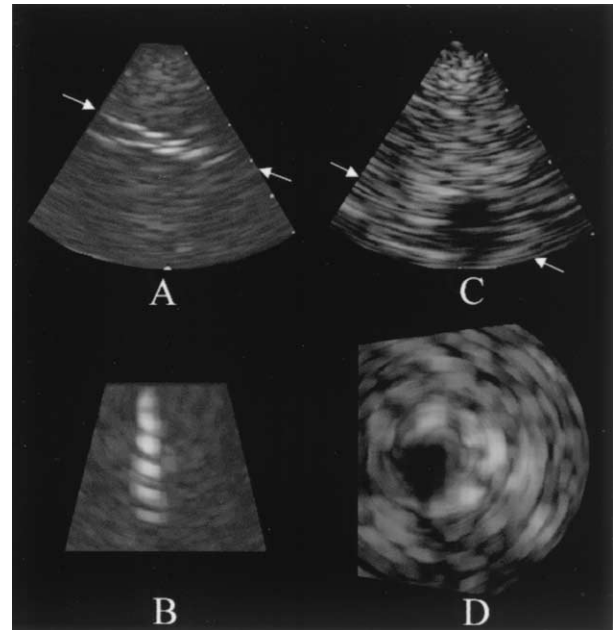


Fig. 8. (A) 6-cm deep B-scan of the CIRS phantom showing “>” shape of the wire targets. (B) Tilted C-scan taken at the plane indicated by the arrows in the B-scans showing wires. (C) 2-cm diameter,  $-20$ -dB contrast cyst in a tissue-mimicking phantom. (D) Tilted C-scan showing cyst.

experiments where interventional devices were introduced through the working lumen of the transducer probe, the device is seen in the central axis of the B-scan images. The identification of the tips of the devices as seen in the US images was verified using x-ray fluoroscopy.

## RESULTS

#### *Transducer characterization*

An illustrative pulse-echo impulse response and spectrum is shown in Fig. 7. The transducer element has a  $-6$ -dB band width of approximately 36% and center frequency of 5.0 MHz. The  $-6$ -dB and  $-20$ -dB pulse widths, indices of axial resolution, are 0.63  $\mu$ s and 1.31  $\mu$ s, respectively.

#### *Images*

*Phantoms.* Figure 8A shows a 6-cm deep B-scan image of the tissue-mimicking CIRS phantom (model 40). The phantom contains two sets of six wires arranged in a “>” shape. The axial spacing of the wires from left to right in the image is 5, 4, 3, 2, 1 and 0.5 mm. From the image, we see that the transducer has axially resolved the 2-mm targets. Figure 8C and D includes a B-scan and tilted C-scan, respectively, of a 2-cm diameter ( $-20$ -dB contrast) cyst at a depth of 5 cm in a tissue-mimicking

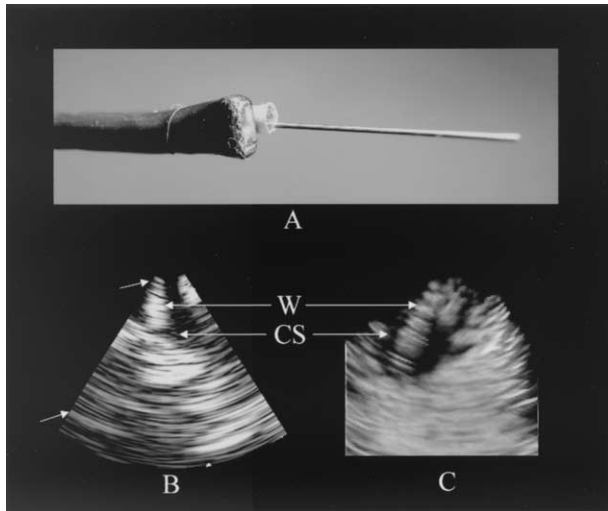


Fig. 9. (A) Photograph of the 14-Fr catheter with 0.36-mm guidewire emerging from tool port. (B) 5-cm deep B-scan showing guidewire (W) being directed into the coronary sinus (CS). (C) Simultaneous 3-D rendered view of the volume of data in between the arrows to the left of the B-scan, showing the guidewire inserted into the coronary sinus.

phantom. The cyst images indicate that the transducer/system should be able to detect important anechoic targets *in vivo*, such as the coronary sinus.

*In vivo manipulation of a guidewire into the coronary sinus.* In a clinically relevant procedure, the 14-Fr catheter was inserted into the jugular vein and advanced prograde into the superior vena cava and then into the right atrium (RA). The coronary sinus (CS) ostium was located and a 0.36-mm (0.014") diameter guidewire was advanced through the working lumen and guided into the coronary sinus. Figure 9A is a photograph of the guidewire emerging from the working lumen of the 14-Fr catheter. Figure 9B and C shows a 5-cm deep B-scan and simultaneous 3-D rendered view of the guidewire being inserted into the coronary sinus. The alignment of the tool port with the imaging catheter along with the combined sector scan and 3-D rendered view eased manipulation of the guidewire into the CS.

*In vivo RV biopsy guidance.* The 14-Fr catheter was further advanced into the RV, and a RV biopsy was performed using a 3-Fr biopsy forceps. Figure 10A is a photograph of the 3-Fr biopsy forceps with jaws in the open position emerging from the working lumen of the 14-Fr catheter. Figure 10B and C shows 3-D rendered volumes of the biopsy forceps (F) in the open and closed positions, respectively, near the RV endomyocardium (E). Guidance of the forceps toward the endomyocardium and confirmation of the open/closed position of the

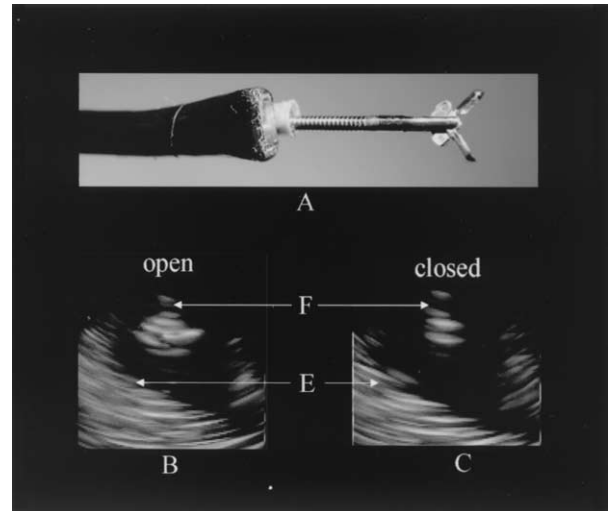


Fig. 10. (A) Photograph of the 14-Fr catheter with 3-Fr biopsy forceps emerging from tool port. (B), (C) 3-D rendered views of the forceps jaws (F) in the open and closed positions, respectively, near the RV endomyocardium (E).

forceps was easily achieved with the forward-viewing dual-lumen transducer.

*In vivo transseptal puncture guidance.* The 22-Fr catheter was inserted into the RA through a small incision that was closed using a pursestring suture. A 71-cm long, 1.27-mm diameter Brockenbrough needle was inserted into the working lumen of the forward-viewing transducer and advanced into the RA. The needle was then used to perform a transseptal puncture so that access to the left atrium (LA) could be obtained. Figure 11A shows a photograph of the needle emerging from the working lumen of the 22-Fr catheter, and Fig. 11B and C shows a simultaneous 6-cm B-scan and 3-D rendered volume of the needle piercing the atrial septum. Visualization of the needle and its guidance across the atrial septum was aided by the forward-viewing dual-lumen transducer.

*In vivo subcutaneous apical four-chamber view.* The 22-Fr catheter was inserted through the skin from a subcostal approach using a surgical trocar, and advanced to the pericardial surface to obtain an apical four-chamber view. Figure 12A is a 10-cm deep 90° B-scan showing all four chambers of the heart. Figure 12B is a 3-D rendered view of the LV and crescent-shaped RV. The 3-D data shown in the images could aid in the placement of pacing leads and assessment of cardiac function during and after surgery.

## DISCUSSION

We have tested the feasibility of using forward-viewing matrix-array catheters to guide interventional

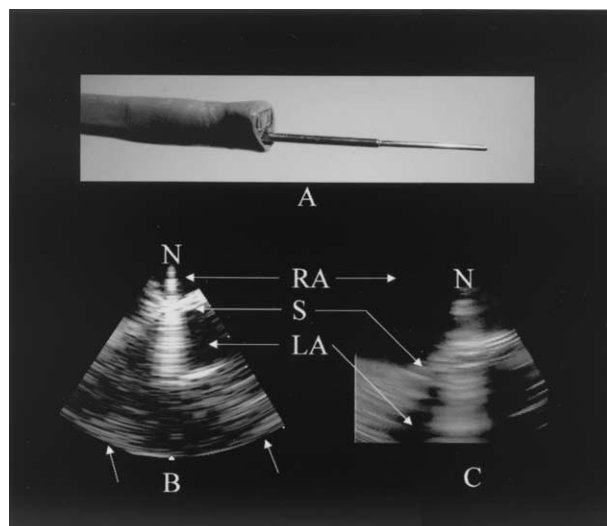


Fig. 11. (A) Photograph of the 22-Fr catheter with Brockenbrough needle emerging from the tool port. (B) 6-cm B-scan of the needle (N) crossing the septum (S) from right atrium (RA) to left atrium (LA). (C) Simultaneous 3-D rendered view of the volume of data in between the arrows beneath the B-scan, showing the needle piercing the atrial septum.

cardiac procedures with RT3-D ICE. The catheters contain a working lumen for interventional tool delivery. We have presented images acquired during *in vivo* interventional procedures, including manipulation of a guidewire into the CS, RV biopsy and transeptal puncture using a Brockenbrough needle. The collinear alignment of the interventional tools with the 3-D imaged volume allows simple, predictable visualization of the tool position and manipulation inside the heart. We have also presented four-chamber images obtained by inserting the forward-viewing probe subcutaneously with a surgical trocar. The

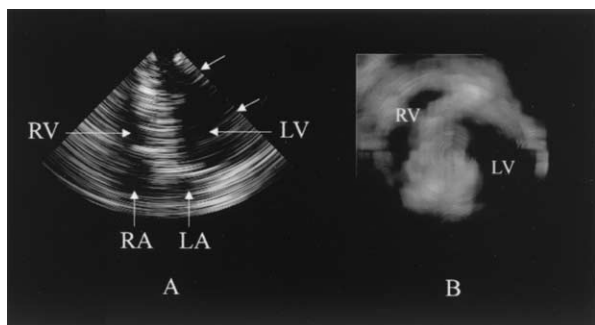


Fig. 12. (A) 10-cm deep apical four-chamber B-scan made with the 22-F catheter in a surgical trocar positioned subcutaneously. Right ventricle (RV), left ventricle (LV), right atrium (RA) and left atrium (LA) are seen. (B) 3-D rendered view of the volume of data in between the arrows to the right of the B-scan showing the LV chamber and crescent-shaped RV.

images may be used to evaluate cardiac function during surgery and postoperatively.

Limitations of the devices mainly revolve around their physical size. The 14-Fr and 22-Fr sizes are too large for routine clinical use. Size reduction could be achieved by using a smaller flex circuit or by, more efficiently, using the available catheter space with custom-extruded dual-lumen catheters instead of juxtaposing two separate catheters. Another limitation is the lack of mechanical steering that would also facilitate clinical use. Nevertheless, the devices demonstrate the potential for simplifying cardiac interventional procedures.

Improvements in image quality can be achieved by utilizing more transducer channels and by utilizing higher-frequency transducers. We have developed transthoracic matrix-array transducers operating at 10 MHz (Light *et al.* 2000), and this technology can be extended to our intracardiac matrix arrays. With these improvements, RT3-D echo using interventional probes could become a valuable clinical tool for simplifying cardiac interventional procedures.

*Acknowledgments*—This research was supported by the NIH (grants HL64962 and HL58754). The authors thank Edward D. Light and E. Dixon-Tulloch for their assistance on this project. They also thank W.L. Gore and Associates for providing the Microflat cables.

## REFERENCES

- Abraham WT, Fisher W, Smith A, *et al.* Long-term improvement in functional status, quality of life and exercise capacity with cardiac resynchronization therapy: The MIRACLE trial experience. *J Am Coll Cardiol* 2002a;39(5, Suppl. A):159A–159A.
- Abraham WT, Fisher W, Smith A, *et al.* Cardiac resynchronization therapy reduces morbidity in patients with moderate to severe systolic heart failure and intraventricular conduction delays. *J Am Coll Cardiol* 2002b;39(5, Suppl. A):171A–171A.
- Ahmad M, Xie TR, McCulloch M, Abreo G, Runge M. Real-time three dimensional dobutamine stress echocardiography in assessment of ischemia: Comparison with two-dimensional dobutamine stress echocardiography. *J Am Coll Cardiol* 2001;37:1303–1309.
- Bartel T, Muller S, Caspari G, Erbel R. Intracardiac and intraluminal echocardiography: Indications and standard approaches. *Ultrasound Med Biol* 2002;28:997–1003.
- Blanc J, Etienne Y, Gilard M, *et al.* Evaluation of different ventricular pacing sites in patients with severe heart failure. *Circulation* 1997; 96:3273–3277.
- Bruce CJ, Packer DL, Seward JB. Intracardiac Doppler hemodynamics and flow: New vector phased array ultrasound tipped catheter. *Am J Cardiol* 1999;83:1509–1512.
- Camarano G, Jones M, Freidlin RZ, Panza JA. Quantitative assessment of left ventricular perfusion defects using real-time three-dimensional myocardial contrast echocardiography. *J Am Soc Echocardiog* 2002;15(3):206–213.
- Caves P, Stinson E, Billingham M, Shumway N. Serial transvenous biopsy of the transplanted human heart: Improved management of acute rejection episodes. *Lancet* 1974;1:821–826.
- Chu E, Fitzpatrick AP, Chin MC, *et al.* Radiofrequency catheter ablation guided by intracardiac echocardiography. *Circulation* 1994;89: 1301–1305.
- Fiering JO, Hultman PA, Lee W, Light ED, Smith SW. High density interconnect for two dimensional arrays. *IEEE Trans Ultrason Ferroelec Freq Control* 2000;47:764–770.

- Fleishman CE, Li J, Ota T, et al. Identification of congenital heart defects using real time three-dimensional echo in pediatric patients. *Circulation* 1996;94(Suppl. I):416.
- Jensen JA, Svendsen NB. Calculation of pressure fields from arbitrarily shaped, apodized, and excited ultrasound transducers. *IEEE Trans Ultrason Ferroelec Freq Control* 1992;39:262–267.
- Lee W, Smith SW. Intracardiac catheter 2-D arrays on a silicon substrate. *IEEE Trans Ultrason Ferroelec Freq Control* 2002;49:415–422.
- Lesh MD, Guerra PG, Roithinger FX, et al. Novel catheter technology for ablative cure of atrial fibrillation. *J Interven Cardiac Electrophys* 2000;4:127–139.
- Light ED, Hultman PA, Idriss SF, et al. Two dimensional arrays for real-time volumetric and intracardiac imaging with simultaneous electrocardiogram. *Proc IEEE Trans Ultrason Sympos* 2000;37121:1195–1198.
- Light ED, Idriss SF, Wolf PD, et al. Real-time 3-D intracardiac echocardiography. *Ultrasound Med Biol* 2001;27:1177–1183.
- McCreery CJ, McCulloch M, Ahmad M, deFilippi CR. Real-time 3-dimensional echocardiography imaging for right ventricular endomyocardial biopsy: A comparison with fluoroscopy. *J Am Soc Echocardiogr* 2001;14:927–933.
- Izutani H, Quan KJ, Biblo LA, Gill IS. Biventricular pacing for congestive heart failure: early experience in surgical epicardial versus coronary sinus lead placement. *Heart Surg Forum* 2002;6(1):E1–6.
- Schmidt MA, Ohazama CJ, Agyeman KO, et al. Real-time three dimensional echocardiography for measurement of left ventricular volumes. *Am J Cardiol* 1999;84:1434–1439.
- Smith SW, Light ED, Idriss SF, Wolf PD. Feasibility study of real-time three-dimensional intracardiac echocardiography for guidance of interventional electrophysiology. *PACE* 2002;25:351–357.
- Smith SW, Pavy HE, von Ramm OT. High speed ultrasound volumetric imaging system Part I: Transducer design and beam steering. *IEEE Trans Ultrason Ferroelec Freq Control* 1991;38:100–108.
- Tsujino H, Jones M, Shiota T, et al. Real-time three-dimensional color Doppler echocardiography for characterizing the spatial velocity distribution and quantifying the peak flow rate in the left ventricular outflow tract. *Ultrasound Med Biol* 2001;27:69–74.
- von Ramm OT, Smith SW, Pavy HE. High speed ultrasound volumetric imaging system part II: Parallel processing and display. *IEEE Trans Ultrason Ferroelec Freq Control* 1991;38:109–115.